Article

Preparation and Electrochemical Properties of Homogeneous Carbon-Coated LiFe$_{0.9}$Mn$_{0.1}$PO$_4$ as Cathode Material for Lithium-Ion Batteries

Yang Xu, Jingang Yu, Sui Peng, Suqin Liu, Zhongqiang Wei, Xianhong Li and Yajuan Li*

College of Chemistry and Chemical Engineering, Central South University, Changsha, 410083, Hunan, P. R. China

Um material catódico homogêneo contendo LiFe$_{0.9}$Mn$_{0.1}$PO$_4$ recoberto com carbono foi sintetizado através de uma reação de etapa única no estado sólido usando glucose como fonte de carbono. Difratometria de raios X de pó (XRD), microscopia eletrônica de transmissão (TEM), voltametria cíclica (CV), espectroscopia de impedância eletroquímica (EIS) e medidas galvanostáticas foram empregadas na caracterização das amostras. A dopagem com manganês e a comodificação com carbono não afetaram a estrutura de olivina do LiFePO$_4$, mas melhoraram a sua cinética em termos da quantidade de energia elétrica fornecida, da polarização e da capacidade de manter uma alta capacitância em altas taxas de carga e descarga. Quando comparado com o LiFePO$_4$/C não-dopado, o LiFe$_{0.9}$Mn$_{0.1}$PO$_4$/C apresentou uma boa distribuição de tamanho – em torno de 100-200 nm – e um desempenho eletroquímico melhor. Em taxas de 0,1, 1,0, 3,0 e 10,0 C (C = 170 mA g^{-1}), o eletrodo LiFe$_{0.9}$Mn$_{0.1}$PO$_4$/C apresentou capacidades de descarga de 154,1, 138,8, 120,0 e 94,0 mA h g^{-1}, respectivamente. Resultados obtidos por voltametria cíclica (CV) e espectroscopia de impedância eletroquímica (EIS) indicaram que a polarização e a resistência de transferência de carga da amostra diminuíram significativamente devido à dopagem com manganês.

Homogeneous carbon-coated LiFe$_{0.9}$Mn$_{0.1}$PO$_4$ cathode material was synthesized by one-step solid-state reaction using glucose as carbon source. Powder X-ray diffractometry (XRD), transmission electron microscopy (TEM), cyclic voltammetry (CV), electrochemical impedance spectroscopy (EIS) and galvanostatic measurements were employed to characterize the samples. Mn-doping and carbon co-modification did not affect the olivine structure of LiFePO$_4$, but improved its kinetics in terms of capacity delivery, polarization and rate capability. When compared with the undoped LiFePO$_4$/C, the LiFe$_{0.9}$Mn$_{0.1}$PO$_4$/C sample presented good size distribution – around 100-200 nm – and better electrochemical performance. At current rates of 0.1, 1.0, 3.0 and 10.0 C (C = 170 mA g^{-1}), the LiFe$_{0.9}$Mn$_{0.1}$PO$_4$/C electrode delivered discharge capacities of 154.1, 138.8, 120.0 and 94.0 mA h g^{-1}, respectively. Results obtained by cyclic voltammetry (CV) and electrochemical impedance spectroscopy (EIS) indicated that the polarization and charge transfer resistance of the sample were greatly decreased by Mn-doping.

Keywords: Mn-doping, LiFePO$_4$, cathode material, lithium-ion batteries

Introduction

Lithium-ion batteries (LIBs) have been widely used in portable electronic devices due to their excellent performance. LIBs are also considered as ideal power supply for electric and hybrid electric vehicles to relieve the pressure from increased oil prices and environmental issues in the future.[1,2] Compared with conventional cathode materials such as LiCoO$_2$, LiMn$_2$O$_4$ and LiNiO$_2$, olivine-type structure LiFePO$_4$ is one of the most promising candidates due to its high theoretical capacity

of 170 mA h g^{-1}, high lithium intercalation voltage of 3.4 V *versus* lithium metal, good thermal stability and long operation life. Most importantly, olivine LiFePO$_4$ possesses other advantages such as environmental benignity and low cost.[3,4] Despite these advantages, olivine LiFePO$_4$ has an intrinsically low electronic conductivity (*ca.* 10^{-9}-10^{-10} S cm^{-1} at room temperature) and low Li$^+$ diffusion rate (*ca.* 1.8 × 10^{-14} cm^2 s^{-1} at room temperature), which may hinder the mobility of electrons and Li$^+$ transport in the electrochemical reaction.[5,6] Numerous efforts have been undertaken to overcome these problems: (*i*) coating with electronically conductive agents (*e.g.* carbon, Cu, Ag),[7,8] (*ii*) ionic doping with foreign atoms to enhance the

*e-mail: yajuanli@csu.edu.cn

electrochemical properties (*e.g.* Mg^{2+}, Zr^{4+}, Cr^{3+})[9-12] and (*iii*) developing synthetic methods to get small particles with well-defined morphology.[13,14]

LiFePO$_4$ can be synthesized by a number of methods, including traditional solid-state reaction, hydrothermal syntheses, sol-gel processing, co-precipitation and microwave methods.[15-19] Recently, solid-state reactions have been considered appropriate for the commercial production of LiFePO$_4$, being also widely used to prepare the highly crystalline olivine-phase LiFePO. Olivine-type LiFePO$_4$ cathode materials were synthesized by a solid-state reaction method and ball-milling.[20] LiFePO$_4$/C, on its turn, was prepared *via* a mechanochemical activation/sintering process using citric acid as carbon source, and showed the discharge capacity of 153 mA h g^{-1} at current rate of 1 C and 92 mA h g^{-1} at 20 C.[21] More recently, Wang *et al.*[22] reported that the rate capability of LiFePO$_4$ can be enhanced by light doping with manganese.

As known, carbon-coating can provide conductive connections between the active particles and create pathways for electron transfer, resulting in an increased electronic conductivity that influences cycling and rate performances.[23] Simultaneously, partial substitution of Mn^{2+} for Fe^{2+} can enhance the mobility of the lithium ions.[22] Constructing LiFePO$_4$ with both carbon-web and ionic doping may be effective to achieve better electrochemical performance. In this work, homogeneous carbon-coated LiFe$_{0.9}$Mn$_{0.1}$PO$_4$ (LiFe$_{0.9}$Mn$_{0.1}$PO$_4$/C) cathode material was synthesized by a solid-state reaction method and ball-milling procedure using glucose as carbon source. Compared with the LiFePO$_4$/C composite cathode, LiFe$_{0.9}$Mn$_{0.1}$PO$_4$/C showed a better electrochemical performance including initial capacity, rate capability, capacity fading and polarization.

Experimental

Synthesis of LiFe$_{0.9}$Mn$_{0.1}$PO$_4$/C and LiFePO$_4$/C

LiFe$_{0.9}$Mn$_{0.1}$PO$_4$/C was synthesized from the starting materials Li$_2$CO$_3$ (99%, AR), FeC$_2$O$_4$·2H$_2$O (99%, AR), Mn(Ac)$_2$·4H$_2$O (99%, AR), (NH$_4$)H$_2$PO$_4$ (99%, AR) and glucose (99%, AR) using a solid-state reaction method. The molar ratio of Li$_2$CO$_3$:FeC$_2$O$_4$·2H$_2$O:Mn(Ac)$_2$·4H$_2$O:(NH$_4$)H$_2$PO$_4$ in the reaction mixture was 0.5:0.9:0.1:1.0. All the starting materials were ball milled for 6 h in a planetary mill with stainless steel vessels and balls, using ethanol as milling medium, ball-to-powder weight ratio of 20:1 and a rotation speed of 300 rpm. Ethanol was removed by evaporation in a blast oven at 60 °C and then the residual mixture was heat-treated in a tube furnace under argon atmosphere at 700 °C for 12 h. Carbon converted from glucose acted as

reducing and conducting agent and its amount was 10 wt.% in the final material. For comparison, the undoped LiFePO$_4$/C composite was also prepared by an identical process except by the addition of Mn(Ac)$_2$·4H$_2$O.

Characterizations

The crystal structure of the samples was characterized by powder X-ray diffractometry (XRD) on a RigaKu D/max 2550VB+ 18 kW equipment using graphite-monochromatized Cu K$_\alpha$ radiation (40 kV, 250 mA). The surface morphology of the samples was observed with a JEM-2010 transmission electron microscope (TEM). The chemical composition was determined with an inductively coupled plasma spectrometer (ICP, Thermo Fisher Scientific, 6500) and with an energy dispersive X-ray spectrometer (EDX) coupled to a JSM-6360-LV scanning electron microscope. The content of carbon was determined by the use of a C-S800 infrared carbon-sulfur analyzer.

The electrochemical properties of the LiFe$_{0.9}$Mn$_{0.1}$PO$_4$/C and LiFePO$_4$/C samples were evaluated with CR2016 coin cells. The cathode was prepared by mixing 80 wt.% of the active material with 10 wt.% acetylene black and 10 wt.% polytetrafluoroethylene (PTFE) emulsion binder. This slurry was pressed on a current collector of aluminum foil (Φ 10 mm) at 15 MPa and dried at 383 K for 12 h in a vacuum oven. The cells were assembled in an argon-filled glove box (Mbraun, Unilab, Germany) using lithium foil as anode, Celgrade® polypropylene as separator and LiPF$_6$ 1 mol L^{-1} in a mixture of EC/DMC/DEC (ethylene carbonate/dimethyl carbonate/diethyl carbonate, volume ratio of 1:1:1) as the electrolyte. Galvanostatic charge-discharge measurements were performed between 2.0 and 4.2 V at room temperature (25 °C) by the use of a LAND battery testing system (CT2001A, Wuhan Land Electronic Co. Ltd., China). Cyclic voltammetry measurements were performed using a CHI660C workstation (Shanghai Chenhua Instrument Co. Ltd., China) at a scan rate of 0.1 mV s^{-1} between 2.5-4.2 V. Electrochemical impedance (EIS) spectra were recorded on a Princeton workstation (PARSTAT2273, EG&G, US) by applying an alternating voltage of 5 mV over the frequency ranging from 0.01 Hz to 100 kHz.

Results and Discussion

Physical properties and morphology

Figure 1a shows the XRD patterns for LiFePO$_4$/C and LiFe$_{0.9}$Mn$_{0.1}$PO$_4$/C. All patterns can be indexed on the bases of an orthorhombic unit cell in space group Pnma, which is
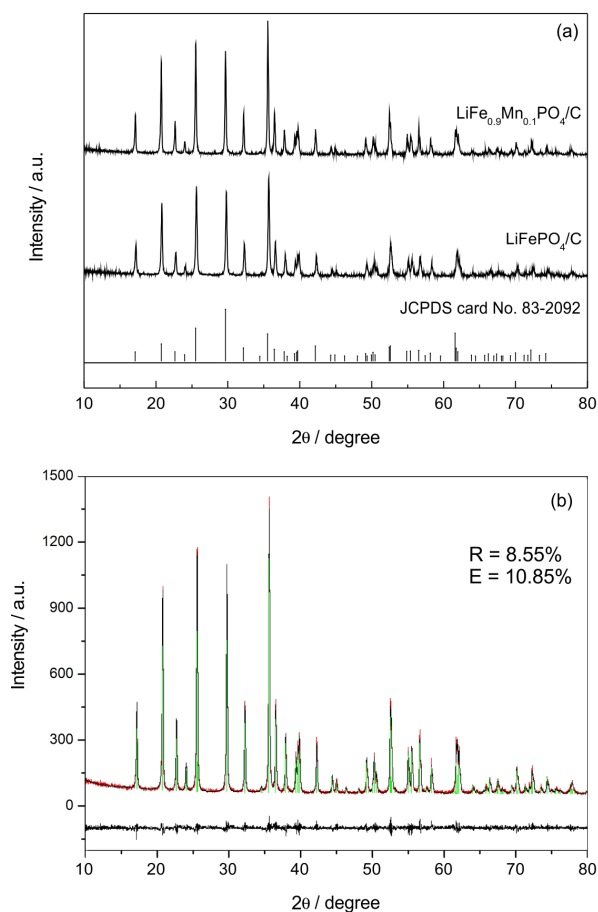
Figure 1. (a) XRD patterns of LiFePO$_4$/C and LiFe$_{0.9}$Mn$_{0.1}$PO$_4$/C and (b) Rietveld refinement of LiFe$_{0.9}$Mn$_{0.1}$PO$_4$/C sample (red dot: observed, black line: calculated and bottom curve: difference).

the same as the standard one (JCPDS card No. 83-2092), and no impurities were detected. Rietveld refinements were carried out by using the Jade 6.5 program for both samples. The typical XRD pattern refinement of LiFe$_{0.9}$Mn$_{0.1}$PO$_4$/C is shown in Figure 1b. Because the correlation R index is less than 10%, and the differences are within error range, the Rietveld refinement results are reliable. It is then possible to indicate that Mn enters the structure of LiFePO$_4$ instead of forming impurities. There is also no evidence for the formation of crystalline or amorphous carbons. The peaks of the LiFe$_{0.9}$Mn$_{0.1}$PO$_4$/C pattern are stronger and narrower than those of LiFePO$_4$/C, indicating the high crystallinity of LiFe$_{0.9}$Mn$_{0.1}$PO$_4$/C. Table 1 shows the lattice parameters of the samples calculated from the XRD patterns. It is observed that the lattice parameters of the two samples are similar to the reported values.[3,24] As shown in Table 1, the unit cell parameters and unit cell volume of LiFe$_{0.9}$Mn$_{0.1}$PO$_4$/C changed a little, *i.e.*, the length of *a*-axis, *b*-axis, *c*-axis and unit cell volume have all increased. Compared with LiFePO$_4$/C, the unit parameters and unit cell volume of LiFe$_{0.9}$Mn$_{0.1}$PO$_4$/C are both expanded, which can be attributed

to the ionic radius of Mn^{2+} (0.97 Å), bigger than that of Fe^{2+} (0.92 Å). The results also indicate that manganese and iron both occupy 4c sites at the tetrahedral Fe environment in LiFe$_{0.9}$Mn$_{0.1}$PO$_4$/C.[25] The expansion in the crystal lattice can provide more space for lithium intercalation/de-intercalation. When Fe^{2+} changes to Fe^{3+} during de-intercalation, the lattice collapses and limits ion diffusion. In the doped LiFe$_{0.9}$Mn$_{0.1}$PO$_4$/C, Mn^{2+} ions in the lattice may act as a pillar to prevent the collapse of the crystals during cycling and thus improve the electrochemical performance.[11,26]

Table 1. Lattice parameters of LiFePO$_4$/C and LiFe$_{0.9}$Mn$_{0.1}$PO$_4$/C

Sample	a / Å	b / Å	c / Å	V / Å^3
LiFePO$_4$/C	10.3191	5.9854	4.6810	289.1170
LiFe$_{0.9}$Mn$_{0.1}$PO$_4$/C	10.3414	6.0035	4.7084	292.3191
Padhi *et al.*[2]	10.3344	6.0083	4.6931	291.4048

TEM images of LiFePO$_4$/C and LiFe$_{0.9}$Mn$_{0.1}$PO$_4$/C are shown in Figure 2. The two samples are composed of small agglomerated particles whose size is in the range of 100-200 nm. Compared with the undoped LiFePO$_4$/C, the LiFe$_{0.9}$Mn$_{0.1}$PO$_4$/C sample has a smaller particle size. TEM analysis confirms a primary crystallite aggregate structure for both LiFePO$_4$/C and LiFe$_{0.9}$Mn$_{0.1}$PO$_4$/C. The crystallite size of LiFePO$_4$/C is obviously larger than the one observed for LiFe$_{0.9}$Mn$_{0.1}$PO$_4$/C. The uniform and small particle size of LiFe$_{0.9}$Mn$_{0.1}$PO$_4$/C will be beneficial to reduce the diffusion length of lithium ion inside the materials, resulting in fast reaction and diffusion kinetics, which can improve charge-discharge capacity and cycling performance. Some uniform carbon-webs are found in the interstitial particle and boundary region (marked with arrows in Figure 2), which are generated from the carbonization of glucose. The carbon webs provide highly conductive channels for the electron mobility among LiFePO$_4$ active particles and enhance the electronic conductivity of the composites.[27] The EDX spectra of LiFePO$_4$/C (Figure 2c) and LiFe$_{0.9}$Mn$_{0.1}$PO$_4$/C (Figure 2d) clearly confirm that the LiFe$_{0.9}$Mn$_{0.1}$PO$_4$/C sample contains Fe, P, O, C and an amount of Mn, while LiFePO$_4$/C does not contain Mn. The atomic ratio of Mn:Fe:P (0.105:0.896:1.000) can be calculated from the EDX pattern. Coupled with the results of the ICP analysis, the real chemical compositions of the LiFe$_{0.9}$Mn$_{0.1}$PO$_4$/C sample is identified as Li$_{0.996}$Fe$_{0.896}$Mn$_{0.105}$PO$_4$/C, which is very close to the designed value.

Electrochemical characterization

Figure 3 shows the initial discharge curves of the LiFePO$_4$/C and LiFe$_{0.9}$Mn$_{0.1}$PO$_4$/C cathodes at current

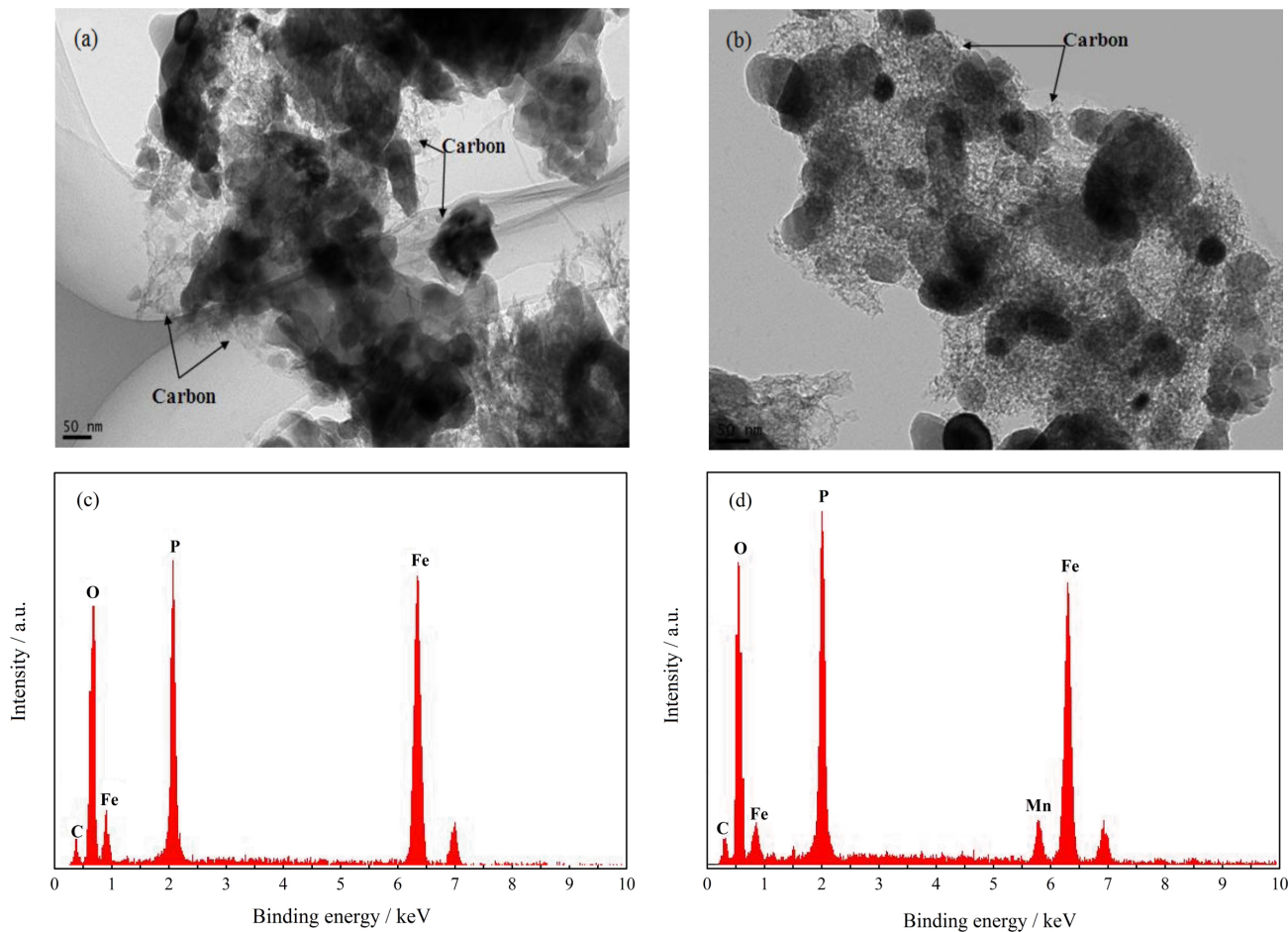**Figure 2.** TEM images of (a) LiFePO$_4$/C and (b) LiFe$_{0.9}$Mn$_{0.1}$PO$_4$/C, and EDX spectra of (c) LiFePO$_4$/C and (d) LiFe$_{0.9}$Mn$_{0.1}$PO$_4$/C.

rates from 0.1 to 10.0 C (C = 170 mA g^{-1}). The cells were tested in two models: (*i*) charged and discharged both at 0.1-1.0 C, as low rate test, and (*ii*) charged at 1 C and discharged at 2.0-10.0 C, as high rate test. There is no observable charge/discharge plateau associated with the Mn^{2+}/Mn^{3+} redox couple in Figure 3b. This indicates that Fe^{2+}/Fe^{3+} is practically the only redox couple that contributes to the electrochemical reaction in the LiFe$_{0.9}$Mn$_{0.1}$PO$_4$/C cathode. It is also observed that the discharge performance of undoped LiFePO$_4$/C is strongly affected by the current density, and its average discharge voltage obviously decreases from 3.40 V (0.1 C) to 2.80 V (10.0 C) with increasing current densities. However, LiFe$_{0.9}$Mn$_{0.1}$PO$_4$/C exhibits an increased initial discharge voltage at all test rates, and the drop of voltage is eased with the increased current densities (3.45 V at 0.1 C and 3.12 V at 10.0 C). This confirms that Mn-doping eases the polarization of the active materials under high current density, and the electrode kinetics of the cathode material is thus improved.[28]
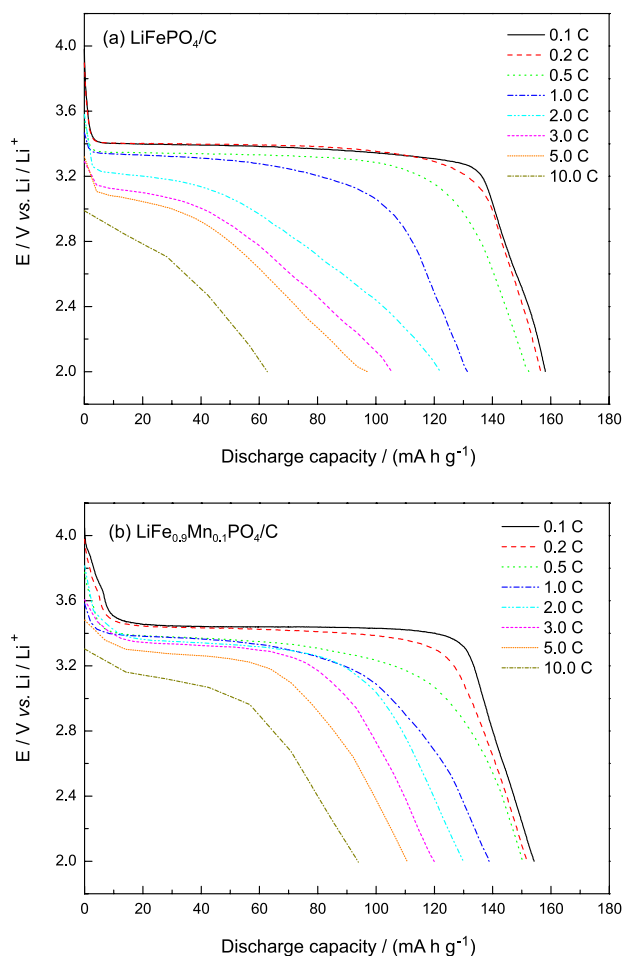
LiFePO$_4$/C delivers a discharge capacity of 158.1 mA h g^{-1} at a low discharge rate of 0.1 C (170 mA g^{-1})

(Figure 3a, Table 2), corresponding to 93% of the theoretical capacity of LiFePO$_4$. LiFe$_{0.9}$Mn$_{0.1}$PO$_4$/C shows a discharge capacity of 154.1 mA h g^{-1} at 0.1 C rate. Since the Mn^{2+}/Mn^{3+} redox couple contributes very little to the capacity, the theoretical capacity of LiFe$_{0.9}$Mn$_{0.1}$PO$_4$/C is reduced to 153 mA h g^{-1}. It is suggested that almost the full Fe^{2+} amount in LiFe$_{0.9}$Mn$_{0.1}$PO$_4$/C is electrochemically utilized at 0.1 C rate, indicating that the utilization of the Fe^{2+}/Fe^{3+} redox reaction is improved with Mn-doping. Furthermore, LiFePO$_4$/C exhibits discharge capacities of 131.5, 105.8, 97.1 and 62.8 mA h g^{-1} at high discharge rates of 1.0, 3.0, 5.0 and 10.0 C, respectively. However, LiFe$_{0.9}$Mn$_{0.1}$PO$_4$/C shows better rate capability as its discharge capacities can reach 138.8, 120.0 and 110.7 mA h g^{-1} at the high discharge rates of 1.0, 3.0 and 5.0 C, respectively. When the current is increased to a rate of 10.0 C, the discharge capacity of the LiFe$_{0.9}$Mn$_{0.1}$PO$_4$/C material can reach the value of 94.0 mA h g^{-1}.

The cycle performances of the LiFePO$_4$/C and LiFe$_{0.9}$Mn$_{0.1}$PO$_4$/C cathodes at various current rates are presented in Figure 4. Due to the limited lithium diffusion and electronic conduction, the discharge capacity
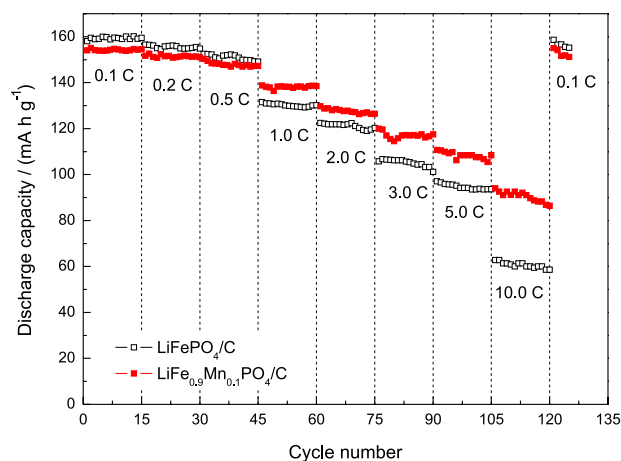
Table 2. The initial discharge capacity of LiFePO$_4$/C and LiFe$_{0.9}$Mn$_{0.1}$PO$_4$/C at current rates of 0.1 to 10.0 C (C = 170 mA g^{-1})

Sample	Current rate / C								
	0.1	0.2	0.5	1.0	2.0	3.0	5.0	10.0	0.2
LiFePO$_4$/C / (mA h g^{-1})	158.1	156.5	152.5	131.5	122.5	105.8	97.1	62.8	156.5
LiFe$_{0.9}$Mn$_{0.1}$PO$_4$/C / (mA h g^{-1})	154.1	151.7	150.3	138.8	129.7	120	110.7	94	151.7

Figure 3. The initial discharge curves of (a) LiFePO$_4$/C and (b) LiFe$_{0.9}$Mn$_{0.1}$PO$_4$/C at various current rates (0.1 to 10.0 C, C = 170 mA g^{-1}) in the voltage range of 2.0-4.2 V (*vs.* Li/Li$^+$).

Figure 4. Cycle performance of LiFePO$_4$/C and LiFe$_{0.9}$Mn$_{0.1}$PO$_4$/C at various current rates (0.1 to 10.0 C, C = 170 mA g^{-1}) in the voltage range of 2.0-4.2 V (*vs.* Li/Li$^+$).

decreased with increasing current rates. LiFe$_{0.9}$Mn$_{0.1}$PO$_4$/C shows better discharge capacity at high current rates than LiFePO$_4$/C. Both samples exhibit good performance on capacity retention because of the carbon-coating. This suggests that the carbon-coating protects the active material from the direct contact with the electrolyte, thus improving the electronic conductivity of LiFePO$_4$.

The electrodes were cycled at 0.1 C after 120 cycles with various current rates. For both samples, full recovery of the discharge capacity is observed at 0.1 C rate even after continuous 10.0 C rate cycles, indicating that the structures of the two samples are very stable during the high rate cycling. The good rate capability of LiFe$_{0.9}$Mn$_{0.1}$PO$_4$/C

can be attributed to the highly uniform distribution of carbon and to the reduced polarization and improved lithium ion diffusion in the lithium intercalation/de-intercalation process induced by Mn-doping.

The effects of Mn-doping on the electrochemical performance of the LiFePO$_4$/C material were further studied by cyclic voltammetry (CV). Figure 5 shows the CV curves of the LiFePO$_4$/C and LiFe$_{0.9}$Mn$_{0.1}$PO$_4$/C cathodes at a scan rate of 0.1 mV s^{-1}. A pair of redox peaks is obviously found in the CV curves, and is related to the two-phase charge-discharge reaction of the Fe^{2+}/Fe^{3+} redox couple. The redox peaks of LiFe$_{0.9}$Mn$_{0.1}$PO$_4$/C are sharper than those of LiFePO$_4$/C. For the LiFePO$_4$/C cathode, the oxidation and reduction peaks center at *ca.* 3.631 and 3.244 V, respectively. The potential separation between the two peaks is 0.387 V. However, in the case of the LiFe$_{0.9}$Mn$_{0.1}$PO$_4$/C cathode, the oxidation and reduction peaks center at *ca.* 3.560 and 3.371 V, respectively, with a potential separation of 0.189 V, less than that observed for LiFePO$_4$/C. This is indicative of small electrode polarization and good kinetics. The potential interval between the oxidation and reduction peaks was used to evaluate the electrochemical reaction reversibility of electrode materials.[29] According to this work, the narrow peak interval and high peak currents indicate the enhancement of the electrode reaction reversibility by carbon-coating and Mn-doping.
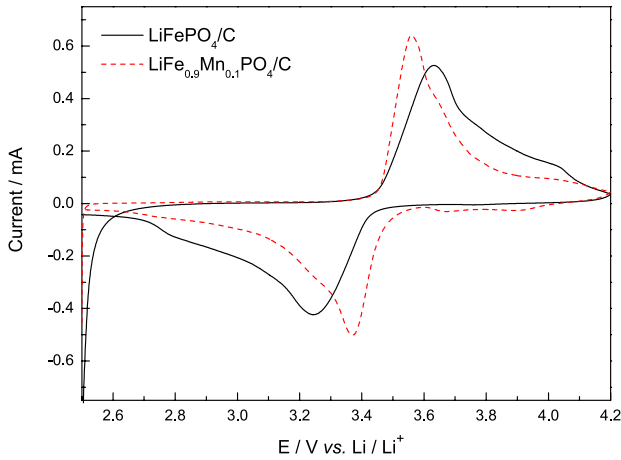
Figure 5. Cyclic voltammograms of LiFePO$_4$/C and LiFe$_{0.9}$Mn$_{0.1}$PO$_4$/C cathodes at a scan rate of 0.1 mV s^{-1}.

In order to estimate the lithium ion diffusion coefficient in the two samples, the electrochemical impedance spectra were registered at room temperature. For this, the cathodes were charged to 3.4 V in the second cycle and then maintained at 3.4 V; typical results are shown in Figure 6a. It is obvious that both spectra are composed of a depressed semicircle in the high frequency and a straight line in the low frequency regions. In Figure 6c, the impedance spectra are fitted with the fitting equivalent circuit model. The intercept at the real impedance axis (Z') identifies the resistance of the electrolyte (R_e). The high frequency semicircle can be assigned to the charge transfer resistance (R_{ct}) and corresponds to the constant phase element (CPE) of the double layer. The sloping line at low frequency can be attributed to the Warburg impedance (W), which is associated with the lithium diffusion in the solid phase. The fitting results of R_e and R_{ct} by the equivalent circuit (shown in Table 3) indicate that the R_{ct} values of LiFe$_{0.9}$Mn$_{0.1}$PO$_4$/C (52.7 Ω) are smaller than that for LiFePO$_4$/C (120.9 Ω). This confirms that the electrochemical activity of LiFePO$_4$/C is improved by doping with a certain amount of Mn^{2+}.

The lithium ion diffusion coefficient D can be calculated according to the following equation:[30]

$$D = \frac{R^2 T^2}{2A^2 n^4 F^4 C^2 \sigma^2} \tag{1}$$

Here R is the gas constant, T the absolute temperature, A the surface area of the electrode, n the number of electrons *per* molecule during the oxidation, F the Faraday constant, C the concentration of lithium ion and σ is the Warburg factor, which is related to Z' by the following, where ω is frequency:[30]

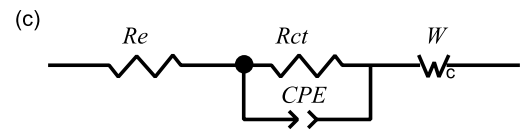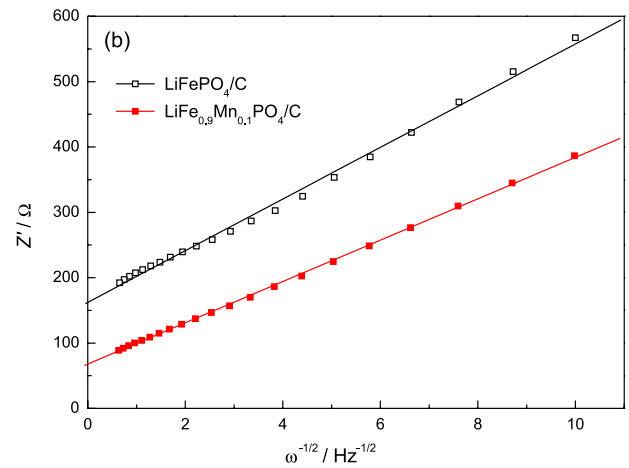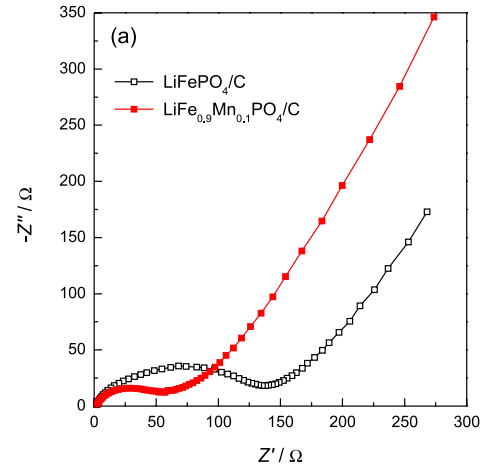$$Z' = R_e + R_{ct} + \sigma\omega^{-1/2} \tag{2}$$

Figure 6. (a) Electrochemical impedance spectra of the LiFePO$_4$/C and LiFe$_{0.9}$Mn$_{0.1}$PO$_4$/C cathodes, (b) the relationship between Z' and $\omega^{-1/2}$ in the low-frequency region and (c) corresponding equivalent circuit model.

Table 3. Fitting results of impedance parameters and lithium diffusion coefficient (D) of LiFePO$_4$/C and LiFe$_{0.9}$Mn$_{0.1}$PO$_4$/C cathodes

Sample	R_e / Ω	R_{ct} / Ω	D / (cm^2 s^{-1})
LiFePO$_4$/C	0.9655	120.9	4.81×10^{-14}
LiFe$_{0.9}$Mn$_{0.1}$PO$_4$/C	1.254	52.7	9.66×10^{-14}

Figure 5b shows the relationship between Z' and $\omega^{-1/2}$ in the low frequency region. The lithium ion diffusion coefficients for both samples are also listed in Table 3. The lithium ion diffusion coefficient is effectively increased by Mn-doping. The decrease in the charge transfer resistance and the increase in the lithium ion diffusion coefficient of LiFe$_{0.9}$Mn$_{0.1}$PO$_4$/C are originated from the increased electronic conductivity and are mainly attributed

to the carbon coating and the larger lattice parameters generated by Mn-doping.

Conclusions

Olivine-structured LiFePO$_4$/C and LiFe$_{0.9}$Mn$_{0.1}$PO$_4$/C composites were successfully synthesized by a solid-state reaction. Powder XRD analysis showed that no impurities were detected and the lattice parameters changed with Mn-doping. Compared with undoped LiFePO$_4$/C, LiFe$_{0.9}$Mn$_{0.1}$PO$_4$/C showed a better electrochemical performance in terms of faster activation, lower electrode polarization and better rate capability, which were attributed to the enhancement of the electronic inductivity by ion doping. At current rates of 0.1, 1.0, 3.0, 5.0 and 10.0 C, the LiFe$_{0.9}$Mn$_{0.1}$PO$_4$/C electrode delivered a discharge capacity of 154.1, 138.8, 120.0, 110.7 and 94.0 mA h g^{-1}, respectively. Results of CV and EIS studies indicated that the combination of Mn-doping and carbon-coating helped to improve the electrochemical properties of LiFePO$_4$.

Acknowledgements

References

1. Bruce, P. G.; Scrosati, B.; Tarascon, J. M.; *Angew. Chem., Int. Ed.* **2008**, *47*, 2930.

2. Mizushima, K.; Jones, P. C.; Wiseman, P. J.; Goodenough, J. B.; *Mater. Res. Bull.* **1980**, *15*, 783.

3. Padhi, A. K.; Nanjundaswamy, K. S.; Goodenough, J. B.; *J. Electrochem. Soc.* **1997**, *144*, 1188.

4. Padhi, A. K.; Nanjundaswamy, K. S.; Masquelier, C.; Okada, S.; Goodenough, J. B.; *J. Electrochem. Soc.* **1997**, *144*, 1609.

5. Chung, S. Y.; Blocking, J. T.; Chiang, Y. M.; *Nat. Mater.* **2002**, *1*, 123.

6. Lu, Z. G.; Cheng, H.; Lo, M. F.; Chung, C. Y.; *Adv. Funct. Mater.* **2007**, *17*, 3885.

7. Bauer, E. M.; Belutto, C.; Pasqual, I. M.; *Electrochem. Solid-State Lett.* **2004**, *7*, 85.

8. Mi, C. H.; Cao, Y. X.; Zhang, X. G.; Zhao, X. B.; Li, H. L.; *Powder Technol.* **2008**, *181*, 301.

9. Wang, D. Y.; Li, H.; Shi, S. Q.; Huang, X. J.; Chen, L. Q.; *Electrochim. Acta* **2005**, *50*, 2955.

10. Yao, J.; Konstantinov, K.; Wang; G. X.; Liu, H. K.; *J. Solid State Electrochem.* **2007**, *11*, 177.

11. Shin, H. C.; Park, S. B.; Jang, H.; Chung, K. Y.; Cho, W. I.; Kim, C. S.; Cho, B. W.; *Electrochim. Acta* **2008**, *53*, 7946.

12. Yin, X. G.; Huang, K. L.; Liu, S. Q.; Wang, H. Y.; Wang, H.; *J. Power Sources* **2010**, *195*, 4308.

13. Wang, Y. G.; Wang, Y. R.; Hosono, E. J.; Wang, K. X.; Zhou, H. S.; *Angew. Chem., Int. Ed.* **2008**, *47*, 7461.

14. Ellis, B.; Kan, W. H.; Makahnouk, W. R. M.; Nazar, L. F.; *J. Mater. Chem.* **2007**, *17*, 3248.

15. Kim, J. K.; Cheruvally, G.; Ahn, J. H.; *J. Solid State Electrochem.* **2008**, *12*, 799.

16. Dokko, K.; Koizumi, S.; Sharaishi, K.; Kanamura, K.; *J. Power Sources* **2007**, *165*, 656.

17. Dominko, R.; Bele, M.; Gaberscek, M.; Remskar, M.; Hanzel, D.; Goupil, J. M.; Pejovnik, S.; Jamnik, J.; *J. Power Sources* **2006**, *153*, 274.

18. Zhou, W. J.; He, W.; Li, Z. M.; Zhao, H. S.; Yan, S. P.; *J. Solid State Electrochem.* **2009**, *13*, 1819.

19. Higuchi, M.; Katayama, K.; Azuma, Y.; Yukawa, M.; Suhara, M.; *J. Power Sources* **2003**, *119-121*, 258.

20. Kang, H.C.; Jun, D. K.; Jin, B.; Jin, E. M.; Park, K. H.; Gu, H. B.; Kim, K. W.; *J. Power Sources* **2008**, *179*, 340.

21. Zhang, D.; Yu, X.; Wang, Y. F.; Cai, R.; Shao, Z. P.; Liao, X. Z.; Ma, Z. F.; *J. Electrochem. Soc.* **2009**, *156*, 802.

22. Wang, X. F.; Zhang, D.; Yu, X.; Cai, R.; Shao, Z. P.; Liao, X. Z.; Ma, Z. F.; *J. Alloys Compd.* **2010**, *492*, 675.

23. Chen, J. M.; Hsu, C. H.; Lin, Y. R.; Hsiao, M. H.; Fey, G. T. K.; *J. Power Sources* **2008**, *184*, 498.

24. Wang, B. F.; Qiu, Y. L.; Li, Y.; *Electrochem. Commun.* **2006**, *8*, 1801.

25. Nakamura, T.; Sakumoto, K.; Okamoto, M.; Seki, S.; Kobayashi, Y.; Takeuchi, T.; Tabuchi, M.; Yamada, Y.; *J. Power Sources* **2007**, *174*, 435.

26. Liu, H.; Cao, Q.; Fu, L. J.; Li, C.; Wu, Y. P.; Wu, H. Q.; *Electrochem. Commun.* **2006**, *8*, 1553.

27. Mi, C. H.; Zhang, X. G.; Zhao, X. B.; Li, H. L.; *Mater. Sci. Eng., B* **2006**, *129*, 8.

28. Tong, D. G.; Luo, F. L.; Chu, W.; Li, Y. L.; Wu, P.; *Mater. Chem. Phys.* **2010**, *124*, 1.

29. Yang, M. R.; Ke, W. H.; *J. Electrochem. Soc.* **2008**, *155*, 729.

30. Bard, A. J.; Faulkner, L. R.; *Electrochemical Methods*, 2nd ed.; Wiley: New York, 2001.